Medical Engineering and Physics 145 (2025) 104422

Contents lists available at ScienceDirect

Medical Engineering and Physics

journal homepage: www.elsevier.com/locate/medengphy

Paper

Comparing fluid dynamics of newborn and adult centrifugal pumps in cardiopulmonary bypass procedures

Silvia Bozzi [a,*], Silvia Colombo [a], Federica Bisconti [a], Paolo Fontanili [b], Marco Corbelli [b], Filippo Consolo [c], Giuseppe Passoni [a], Alberto C.L. Redaelli [a]

[a] Department of Electronics, Information and Bioengineering, Politecnico di Milano, Piazza Leonardo da Vinci 32, 20133 Milan, Italy
[b] Eurosets S.r.l., Strada Statale 12, n°143, 41036 Medolla MO, Italy
[c] Università Vita Salute San Raffaele, Via Olgettina 58, 20132 Milan, Italy

ARTICLE INFO

Keywords:
Extracorporeal circulation
Cardiopulmonary bypass
Neonatal application
ECMO
Levitating centrifugal pumps
Newborn patients
Computational fluid dynamics
Blood damage
Thrombogenicity

ABSTRACT

Background: Cardiopulmonary bypass (CPB) plays a crucial role in cardiac surgery, with the pump being a key component affecting both hemolysis and thrombosis. Centrifugal levitating pumps (CP) have demonstrated superiority over roller pumps due to reduced hemolysis, but thrombotic risk remains a concern. Nonetheless, there exists a technological gap for newborn patients, with only two approved centrifugal pumps specifically tailored for their needs. Consequently, pumps originally designed for adults are often employed as substitutes for paediatric patients. However, the mismatch between pump characteristics and paediatric physiology can lead to issues like blood dilution, increased shear stress, and suboptimal performance.
Methods: This study investigates the hemodynamics of an adult CP compared to a downscaled newborn CP featuring a 40% reduction in priming volume. Computational fluid dynamics is used to assess differences in flow characteristics, shear stresses, and stagnation zones, with implications for blood damage and thrombogenicity.
Results and conclusion: The newborn pump features notably shorter exposure times (45% lower than the adult design), reduced peak stress values, and a 20% reduction in the volume of fluid exposed to stress levels exceeding 50 Pa, suggesting a potential decrease in the risk of blood damage. Additionally, its reduced extent of stagnation zones (0.13 ml compared to 0.21 ml) indicates improved washout performance, thus lowering the risk of platelet aggregation and thrombus formation. These findings suggest that using a paediatric pump instead of an adult pump at typical flow rates for newborn patients may reduce the risk of blood damage.

1. Introduction

In cardiopulmonary bypass (CPB) the pump is the crucial component for its implications on both hemolysis and thrombosis. Since the work by Sasaki et al. [1], the superiority of centrifugal pumps (CP) over previous roller pumps (RP) has been acknowledged, especially for tests prolonged beyond usual CPB duration [2]. The advantages of CP over RP in paediatric patients have been debated over many years since the work by Morgan et al. [3], which proved reduced cellular damage with CP in terms of lower haemolysis and maintenance of platelet and leukocyte counts.

CP performances have been substantially further improved by taking the advantage of magnetic levitation (ML) of the impeller. This technique avoids solid contact among the moving parts and reduces associated blood damage, as shown in early animal experiments by Taenaka et al. [4] and confirmed in manifold subsequent studies demonstrating that ML adult pumps can substantially reduce hemolysis [5–8].

The increasing use of mechanical circulatory support systems in clinical practice has posed new questions on the interaction between artificial devices and blood structure. Beyond hemolysis, the thrombotic risk assessment, has emerged as a new benchmark [9]. Indeed, thrombosis was - and still is – a major concern in CP since thrombi tend to form in specific locations where shear and temperature effects are magnified, particularly close to metal shaft bearings and, to a minor extent, along the upstream portion of the vanes. This phenomenon has been observed in both clinical Extracorporeal Membrane Oxygenation (ECMO) circuits and in-vitro flow loop studies with porcine whole blood [10].

* Corresponding author at: Department of Electronics, Information Science, and Bioengineering, Politecnico di Milano, Piazza Leonardo da Vinci 32, 20133 Milano, Italy.
E-mail address: silvia.bozzi@polimi.it (S. Bozzi).

https://doi.org/10.1016/j.medengphy.2025.104422
Received 25 November 2024; Received in revised form 30 May 2025; Accepted 25 August 2025
Available online 25 August 2025
1350-4533/

Thrombotic risk is enhanced by high shear stresses and exposure times [11]. Conversely, it has been demonstrated that the reduction of the recirculation ratio in a ML pump, obtained through small scale optimization, limits the thrombotic risk [12].

The effect of pump gaps design on hemolysis damage has been investigated by Graefe et al. [13] through numerical simulation. Mozafari et al. [14] showed how normalized hemolysis index is inversely correlated with pump efficiency concerning the number of blades and the outlet width. More extensively, Wiegmann et al. [15] explored the controversial impacts of gaps, blades and shroud on pump efficiency and hemolysis-thrombosis indicators. Accurate numerical simulations have also been used by Berg et al. [16] to identify the locations of intense vortical structures, commonly associated with clot formation. Bozzi et al. [17] showed how shear stress, shear rate, exposure time and platelet activation are affected by the number of blades of the pump. A multi-objective numerical optimization of blades and volute geometry has been the goal pursued by Huang et al. [18] to minimize the hemolysis index.

More recently, ML technology has been applied in paediatric surgery, resulting in improved clinical outcomes compared to standard CP, in terms of both end-organ recovery and long-term survival rates [19,20]. However, only two pumps specifically designed for newborn applications are now commercially available (Pedivas® by Levitronix, Zurich, Switzerland and Deltastream DP3 by MEDOS Medizintechnik AG, Stolberg, Germany) despite adult centrifugal blood pumps, while effective in adults, pose challenges when applied to paediatric patients. The mismatch between adult pump characteristics and paediatric physiology results in suboptimal performance, significant hemodilution and increase use of packed red blood cells, due to the high priming volume of the CPB circuit. Moreover, using an adult-size centrifugal blood pump in paediatric circuits also leads to higher shear stress and hemolysis [21] along with increased platelet activation as recently demonstrated by Fiusco et al. [22] in their comparison of the thrombogenicity of a paediatric and an adult pump. To address these challenges, there is a growing emphasis on the development of blood pumps specifically tailored to the needs of neonatal and paediatric patients. These pumps are designed with reduced volume capacities to minimize blood dilution, a critical factor in maintaining appropriate haematocrit levels in small patients. Additionally, they are optimized to operate efficiently at lower flow rates, ensuring compatibility with the lower cardiac outputs typical of paediatric cases.

Due to the limited number of investigations on paediatric devices, the effect of CP downscaling and its influence on device thrombogenicity have been investigated in this paper. Specifically, computational fluid dynamics (CFD) simulations were employed to compare the reliable ECMOLife adult pump by Eurosets [7,23] with the newly designed Eurosets newborn pump (New Born ECMOLife), which features a 40% reduction in priming volume and has been tested at low flow rates on healthy young swines resulting in good haemodynamic performance [24]. To understand the fluid dynamics of the neonatal pump, we simulated two operational conditions representing flow rates of 0.5 l/min and 1 l/min, while for the adult pump, we simulated its operation at the most clinically relevant neonatal condition, i.e., 0.5 l/min flow rate. To compare the risk of blood damage between adult and neonatal pumps, we performed thorough qualitative and quantitative evaluations of the flow fields measuring stagnation zones, investigating flow disturbances, and quantifying areas with critical fluid stress values.

2. Materials and methods

2.1. Geometry and mesh

Eurosets pumps for adults and newborn patients have the same design but different sizes. The adult pump has 3/8-inch inlet and outlet, a six-blades impeller with an outer diameter of 49 mm and a priming volume of 39 ml. The newborn Eurosets pump has 1/4-inch inlet and outlet, a six-blades impeller with an outer diameter of 41 mm and 22 ml priming volume.

The geometrical model of the newborn pump was created with ANSYS® SpaceClaim 22.2 (ANSYS Inc., Canonsburg, PA, USA) starting from the CAD rendering provided by Eurosets S.r.l. The device consists of four main components: impeller, upper housing, lower housing and seal, that were combined in two components (housing and impeller) for the subsequent meshing process (Fig. 1a). Two additional geometry modifications were also introduced: (1) the impeller was raised by 2 mm with respect to the rest condition to simulate the effective levitated position measured experimentally and (2) inlet and outlet ducts were extended by a length equal to 10 times the diameter of the inlet pipe, to guarantee a developed flow, in agreement with the experimental setup, used to measure pressure heads. To apply the sliding mesh approach, the fluid domain was divided in two sub-volumes: the rotor, consisting of the rotating fluid volume surrounding the impeller and the stator, i.e., the static fluid volume contained within the volute. The interface between the two fluid domains was placed halfway between the impeller side and the volute wall.

The computational mesh adopted in this study was derived from a previously published CFD analysis of the same adult Eurosets pump [17], for which a comprehensive mesh convergence study was conduct-ed. For the neonatal pump, the same meshing strategy was applied after appropriate geometric rescaling to preserve the relative element distribution and ensure consistency in numerical accuracy. Hexahedral elements of 270 μm size were used to discretize the lower part of the pump, i.e., the bottom and the sides of the stator and rotor, introducing at least five layers of elements into the smallest gaps (Fig. 1b). The rest of the domain, excluding the region surrounding the blades, was discretized with tetrahedral elements of size of approximately 270 μm. Local mesh refinement was performed in proximity of the blades using tetrahedral elements of size equal to 126 μm, comparable with the Taylor scale. The final grid contained 15.7 million cells.

2.2. Fluid dynamics simulations

The flow field was resolved using the finite volume solver ANSYS® Fluent 22.2 (ANSYS Inc., Canonsburg, PA, USA). The three-dimensional unsteady Navier-Stokes equations were solved with a Direct Numerical Simulation (DNS) approach without any turbulence model. This was possible since the accuracy in the discretization adopted here was coherent with indications in Moin and Mahesh [25] and similarly to centrifugal pump simulations by Berg et al. [16] and Bozzi et al. [17]. In CPs the domain scales are close to large vessels and the expected velocities are much larger than the physiological ones, hence non-linearities in the rheological model do not give a significant contribution [26,27]. The blood was then assumed to behave like a Newtonian fluid with density 1060 kg m^{-3} and dynamic viscosity 0.003 Pa•s. The numerical solution was obtained using the SIMPLE algorithm for pressure-velocity coupling and an implicit second-order temporal and spatial discretization. A convergence criterion of 10^{-5} was set for the residual errors of continuity and momentum equations. The time step was set equal to the time required for a 2° rotation of the impeller. The rotation of the impeller was implemented as a rigid body motion, using a sliding mesh approach. A mass flow rate was imposed at the inlet pump and a zero-pressure gradient was prescribed at the outlet. Simulations were run for three complete rotations of the impeller to achieve a stationary periodic solution, and the fourth cycle was used for the analysis.

To characterize the fluid dynamics of the neonatal pump, two operating points (NB_WP1 and NB_WP2) were simulated, corresponding to flow rates of 0.5 L/min and 1.0 L/min, respectively. These values represent typical clinical conditions encountered in neonatal extracorporeal circulation, as reported by Meyer et al. [28]. Based on the flow rate–rotational speed curves, the corresponding rotor speeds were set to 2500 rpm and 3500 rpm, respectively. For comparison, the adult pump was simulated only at the most clinically relevant neonatal operating

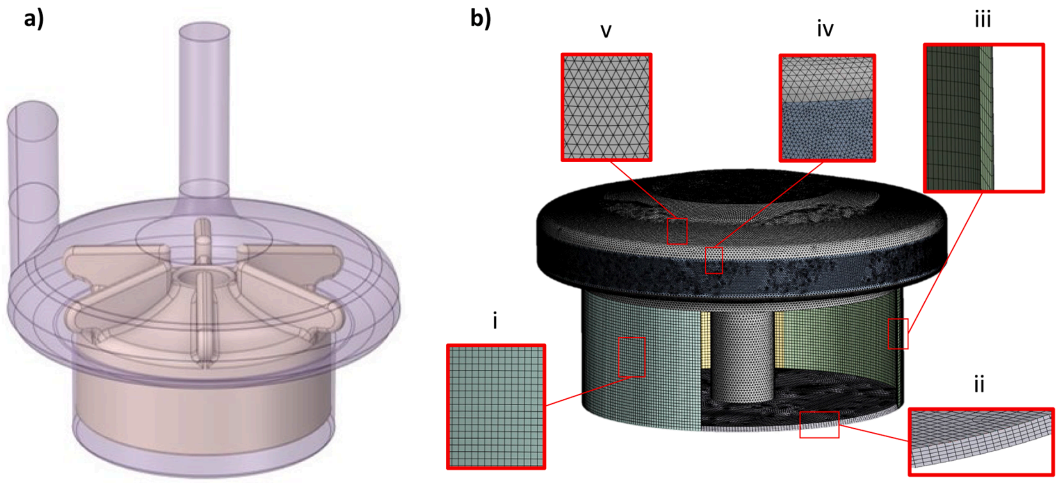

Fig. 1. Details of the pump geometry and mesh: a) 3D CAD drawing of the newborn pump showing the housing (violet) and the impeller (beige); b) mesh of the rotor region: i) lateral surface, hexahedral cells 270 μm; ii) bottom gap, 5 layers hexahedral cells 270 μm; iii) lateral gap, 5 layers hexahedral cells 270 μm; iv) blades region, tetrahedral cells 126 μm; v) impeller, tetrahedral cells 270 μm.

point, i.e., 0.5 L/min (A_WP1), with a corresponding rotor speed of 2280 rpm. In all cases, the mass flow rate was imposed at the inlet pump and a zero-pressure gradient was pre-scribed at the outlet, assuming fully developed flow conditions. Regarding initial conditions, a zero-velocity field was imposed across the domain. Simulations were run for three full impeller rotations to ensure convergence to a periodic steady-state regime. Data from the fourth rotation were then used for the quantitative analyses.

Simulations were run on a Server Rack FUJITSU PRIMERGY RX300S7 equipped with an Intel® Xeon® Gold 6148 processor with 40 computational cores (clock frequency of 2.40 GHz, shared RAM of 96 GB). The CPU time was about 7 days for each simulation.

Results were compared in terms of flow fields, stagnation zones and fluid stress levels. Stagnation zones, which represent potential risk of thrombus formation, were defined as regions with velocity magnitude lower than 0.5 m/s according to Wiegmann et al. [15]. The risk of shear-mediated platelet activation was assessed by evaluating wall shear stress and the scalar stress σ, calculated using the formula proposed by Bludszuweit [29]:

$$\sigma = \left(\frac{1}{12}\left(\tau_{ii} - \tau_{jj}\right)^2 + \frac{1}{2}\tau_{ij}^2\right)^{1/2} \tag{1}$$

where each value of τ_{ij} represents a component of the deviatoric part of the total stress tensor, while the isotropic part of the full stress tensor has a null contribution.

Since platelet activation depends on both the magnitude and duration of shear stress exposure [30,31], and no universally accepted threshold exists, we presented the full volumetric distribution of scalar shear stress and focused on two threshold values (50 Pa and 100 Pa) to enable a quantitative comparison between the two pumps. In addition, we visualized areas with wall shear stress exceeding 100 Pa and volumes of fluid above this threshold to highlight the most critical regions within the flow field.

2.3. Validation

To validate the numerical results, the hydraulic performance of the adult and neonatal pumps was experimentally assessed using a mock loop (Fig. 2) in accordance with ISO 18242:2016 [32]. A blood analog was prepared using a distilled water–glycerol mixture, consisting of 37.5% by volume of 99.5% pure glycerol, resulting in a fluid with a dynamic viscosity of 0.003 Pa·s. The mixture was then placed in a rigid polycarbonate reservoir with a total volume of 4500 mL, connected to a

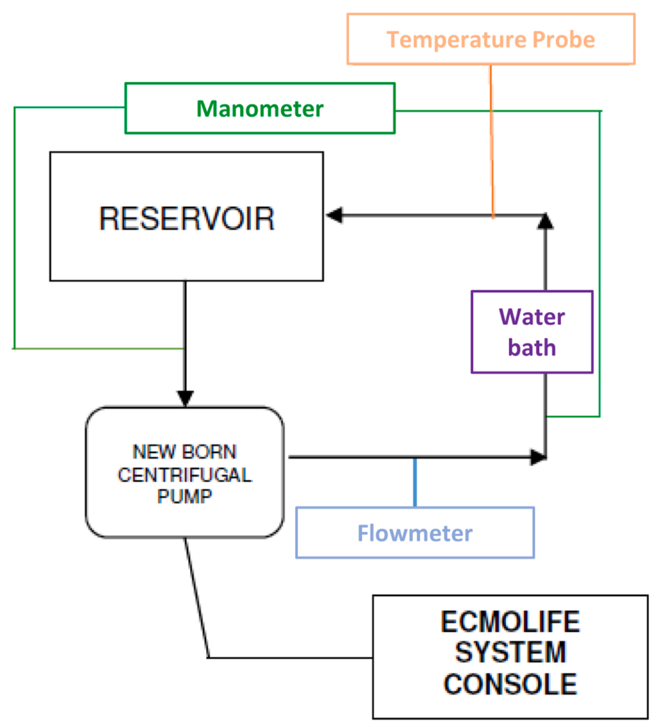

Fig. 2. Experimental mock loop used for the characterization of the pumps.

circuit using either 3/8” or 1/4” inner diameter PVC medical tubing for the adult and newborn pumps, respectively. To change the flow resistance, the hydraulic afterload was adjusted by partially constricting the outlet tubing. Flow rates were measured using an in-line ultrasonic flow probe (EMTEC SONO), while pressure differential across the pump was acquired via a pressure transducer (KIMO CP115-AO). All experiments were conducted at 37°C using a thermoregulated water bath (Thermo Electron Corporation).

3. Results

3.1. Validation

Fig. 3 shows the characteristic curves of the adult pump (a) and the

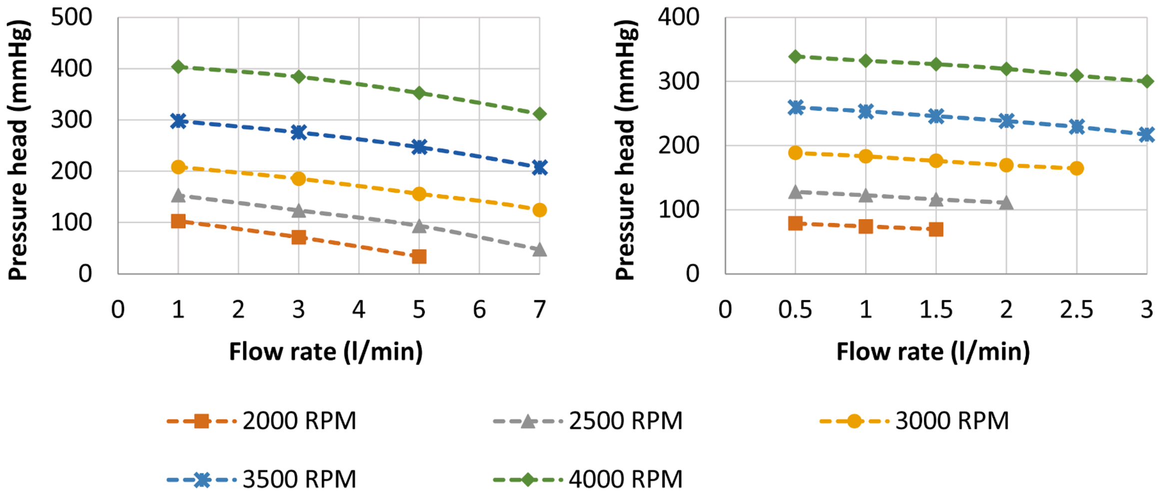

Fig. 3. Characteristic curves of the adult (a) and newborn (b) pumps. The graphs illustrate the relationship between pressure head and flow rate at various rotational speeds.

Newborn pump (b), while Table 1 summarizes the experimental and numerical results for head generation. The comparison indicates that the simulations reliably predict head generation across all cases, with relative percentage errors ranging from 2% for the adult pump to 5% for the newborn pump at the operating flow rate of 0.5 l/min.

3.2. Flow field

Fig. 4 depicts contour maps of relative velocity magnitude (with respect to the rotating coordinate system) for both the adult pump (A_WP1) and the newborn pump at the two distinct operating points (NB_WP1 and NB_WP2). Observable flow features include low velocities in the inlet pipe and small gaps between the rotor and stationary housing, with velocity increasing in the outermost part of the volute due to the propulsive action of the blades. Blood entering from the inlet accelerates radially along the blades under centrifugal force, reaching maximum speed at the trailing edges of the blades before exiting through the tangential outlet.

Comparing the newborn and adult pumps at the same operating point reveals lower blood velocity in the suction line of the adult pump due to its larger inlet pipe diameter. However, the volute exhibits higher speeds and larger vortexes in the adult pump, despite its lower rotational speed. This discrepancy arises from the adult pump's larger rotor radius and blade size, which provide greater fluid propulsion. Additionally, the washout hole of the neonatal pump facilitates faster fluid movement, promoting increased recirculation.

Comparing the two operating conditions of the newborn pump illustrates that higher rotor speed enhances blood recirculation in the small gaps between the rotor and stationary housing.

Table 1
Pump characteristics and comparison of experimental and numerical results.

	Adult pump (A)	Newborn Pump (NB)	
	WP1	WP1	WP2
Fluid volume [ml]	39	22	22
Rotor diameter [mm]	49	41	41
Speed [rpm]	2280	2500	3500
Flow rate [l/min]	0.5	0.5	1
Numerical head generation [mmHg]	126	122	242
Experimental head generation [mmHg]	128	128	253
Difference [%]	2%	5%	4%

3.3. Flow stagnation

Fig. 5 illustrates flow stagnation zones, where the risk of platelet aggregation and thrombus formation arises due to blood cell stasis. These regions are notably observed in the small gaps between the rotor and stationary housing, the washout hole, and at both the pump outlet and inlet. Both the adult and newborn pumps exhibit similar distributions of stagnation zones, but the extent is significantly greater in the adult pump: 0.21 ml compared to 0.13 ml (Table 2). This discrepancy primarily stems from the larger volume of fluid within the adult pump, coupled with the lower rotational speed of the rotor, resulting in decreased velocities in regions not directly affected by the propulsive action of the blades. Regarding the newborn pump, as the flow rate increases from 0.5 L/min to 1 L/min, stagnation zones reduce and become confined primarily to the inlet duct.

3.4. Fluid stresses

Fluid stresses are represented in Fig. 6 and Fig. 7, showing respectively wall shear stress (WSS) and scalar stress across various regions of the pumps. Table 2 reports fluid dynamics parameters associated with blood damage and thrombus formation.

In all the simulations, the maximum shear stress occurs at the trailing edges of the blades (Fig. 6, first line), where the fluid experiences the highest velocity gradients. The peak WSS is equal to 482 Pa in the adult pump, 334 Pa in the newborn pump under the same working condition and 533 Pa in the newborn pump at a flow rate of 1 l/min.

To highlight the most critical regions with regards to blood damage, surface areas with wall shear stress exceeding 100 Pa were visualized and quantified (Fig. 6, second and bottom lines). These areas exhibit a similar distribution in both the adult and newborn pumps, primarily located at the trailing edges of the blades, along the side walls of the rotor, and on the volute wall. In the adult pump, surface areas characterized by WSS above 100 Pa measure 16 cm^2, whereas in the newborn pump at the same operating condition, it measures 11 cm^2. A larger critical area is evident in the adult pump, particularly along the blade tips of the rotor, as depicted in Fig. 6. In the newborn pump, the wall area with shear stress above 100 Pa triples from 11 cm^2 to 39 cm^2 when the flow rate doubles.

Contour maps of scalar stress in the rotor plane reveal that stress levels are elevated at the suction side of blades, due to the presence of vortex structures within the impeller wake (Fig. 7, top line). In the adult pump, larger gaps result in more pronounced flow disturbances along the fluid path, leading to higher values of scalar stress compared to the

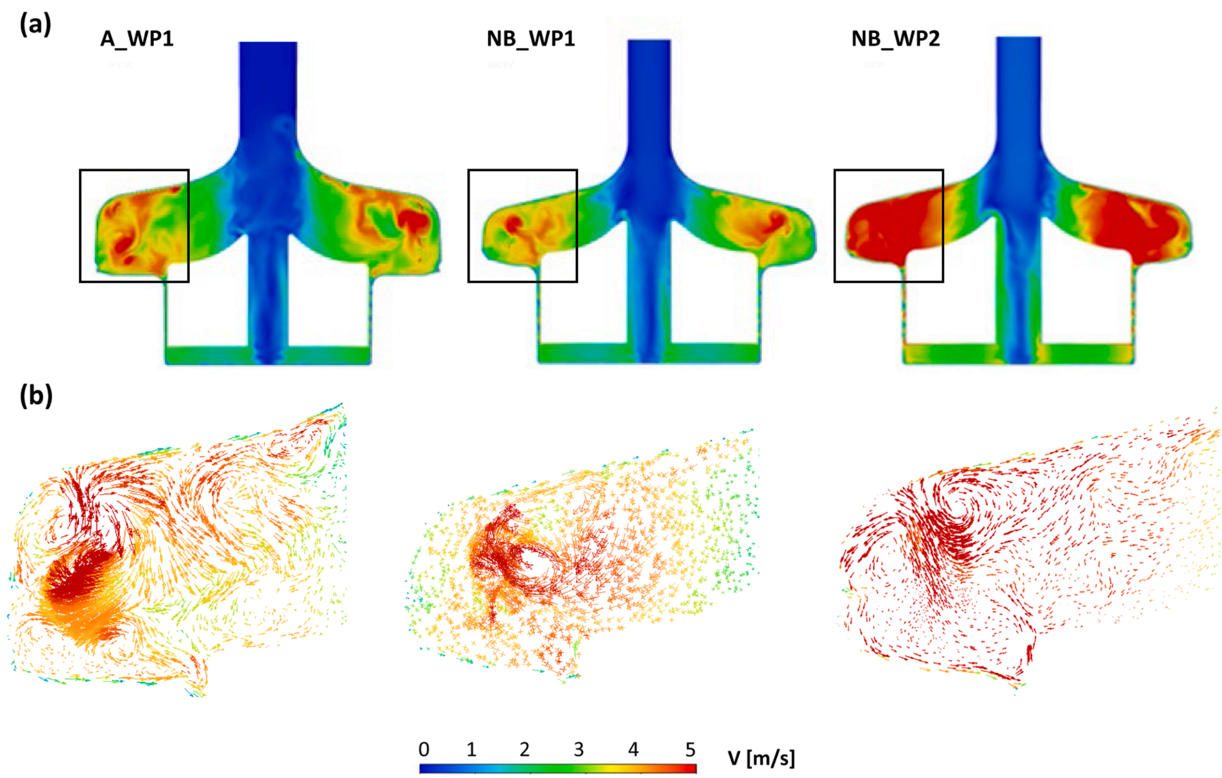

Fig. 4. Contour maps of velocity magnitude [m/s] (a) and velocity vectors (b): comparison between A_WP1 (adult pump at working point WP1), NB_WP1 (newborn pump at working point WP1) and NB_WP2 (newborn pump at working point WP2). The square shown in the contour maps indicates the region where the velocity vectors are visualized.

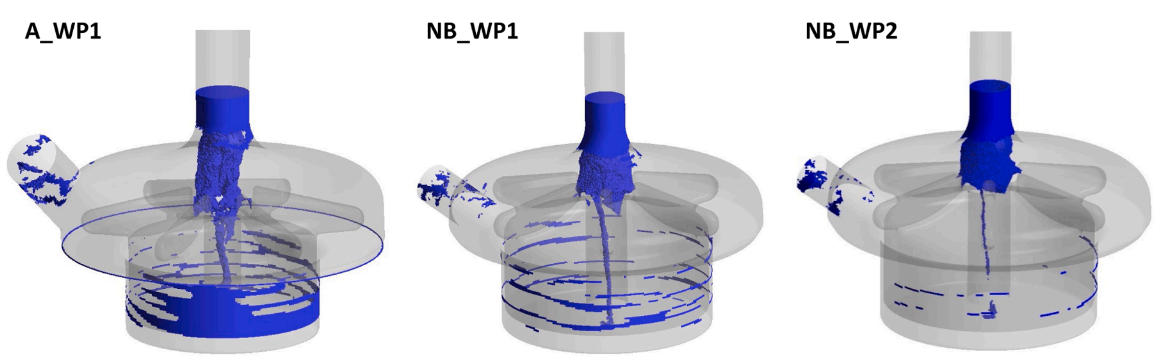

Fig. 5. Stagnation zones: comparison between A_WP1 (adult pump at working point WP1), NB_WP1 (newborn pump at working point WP1) and NB_WP2 (newborn pump at working point WP2).

Table 2
Blood damage related fluid dynamics parameters.

	Adult Pump (A)	Newborn Pump (NB)	
	WP1	WP1	WP2
Eulerian integral time scale V/Q [s]	4.7	2.6	1.2
Fluid volume with velocity magnitude below 0.5 m/s [ml]	0.21	0.13	0.11
Area of wall shear stress above 100 Pa [cm^2]	16	11	39
Maximum wall shear stress [Pa]	482	334	533
Maximum scalar stress [Pa]	395	254	437
Fluid volume with scalar stress above 50 Pa [ml]	0.47	0.37	0.83
Fluid volume with scalar stress above 100 Pa [ml]	0.08	0.05	0.34

newborn pump.

Fig. 8 presents the volumetric histograms of the scalar stress of the adult and newborn pumps, specifically focusing on values above 10 Pa. The distributions show that in the adult pump, larger volumes of fluid are exposed to scalar stresses above 50 Pa, amounting to 0.5 ml, compared to 0.4 ml in the newborn pump. When considering the threshold value of 100 Pa, the difference becomes larger, with the newborn pump exhibiting 40% less volume above this value.

4. Discussion

This study aimed to evaluate and compare the fluid dynamics of a centrifugal pump specifically designed for newborns with a standard adult centrifugal pump operating under pediatric CPB conditions, i.e., at low flow rates. Through computational fluid dynamics, we investigated parameters known to influence blood damage and thrombogenicity - namely, shear stress exposure, blood residence time, and the presence of

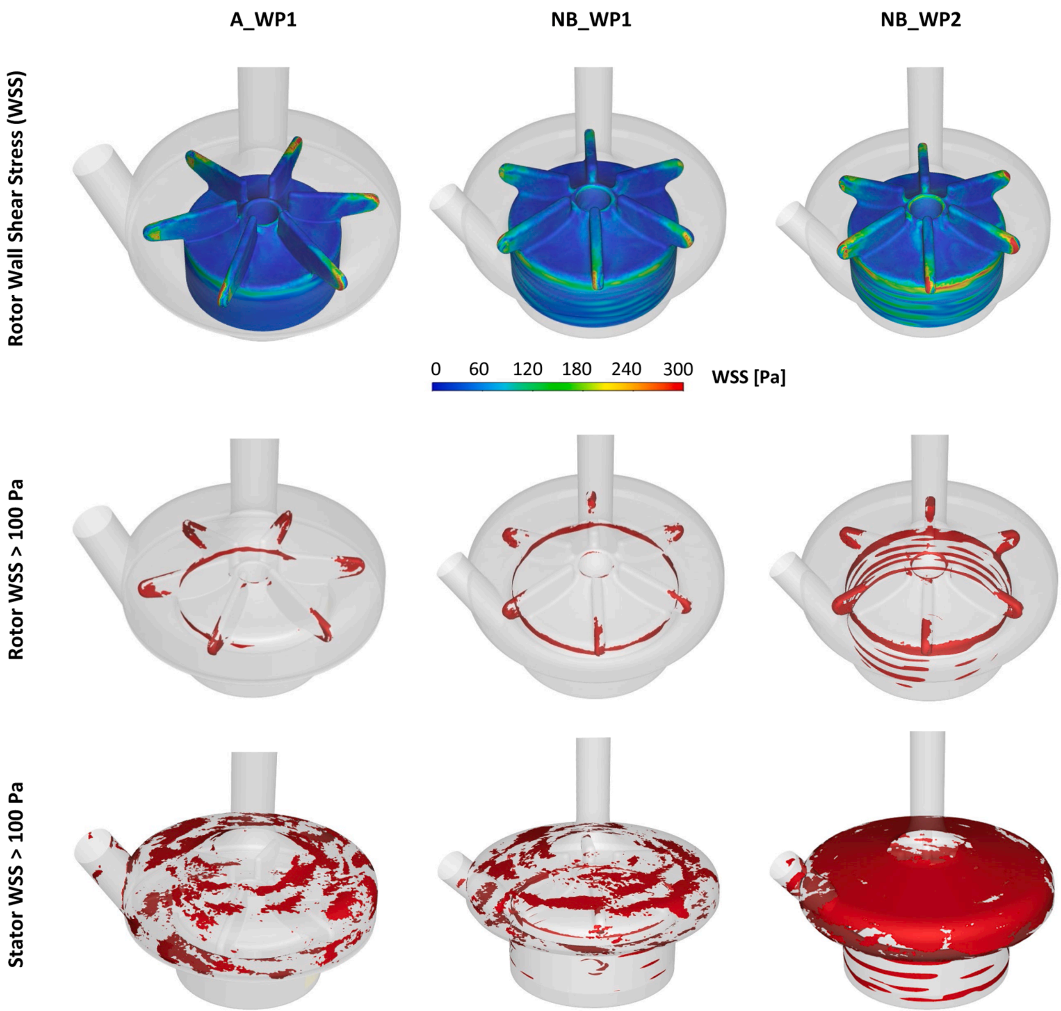

Fig. 6. Contour maps of wall shear stress (WSS) on the rotor surface (top row) and surface area of the rotor (middle row) and the housing (bottom row) with WSS above 100 Pa: comparison between A_WP1 (adult pump at working point WP1), NB_WP1 (newborn pump at working point WP1) and NB_WP2 (newborn pump at working point WP2).

stagnation zones.

Our results highlight several important differences between the two pump designs. The adult pump, due to its larger internal volume and wider gaps, generates more prominent flow disturbances and larger vortical structures. Besides the negative impact of the larger gaps, the adult pump exhibits higher flow velocities at the blade trailing edges—and consequently along the adjacent volute walls—due to its larger blade radius, despite operating at a lower rotational speed than the neonatal pump. These regions of elevated wall shear stress are known to correlate with increased risk of platelet activation and hemolysis, as discussed in previous literature [18,22,29].

In terms of scalar stress distributions, the fluid volume exposed to high stresses (i.e. $>$ 50 Pa) is 25% higher in the adult pump. When considering a more severe threshold value of 100 Pa, the discrepancy increases further, with the adult pump exposing 70% more fluid volume to such stresses. Notably, residence time in the adult pump is also significantly longer—about 80% higher—indicating prolonged exposure of blood cells to mechanical stresses. Since both shear magnitude and duration are known contributors to hemolysis and thrombogenic risk, these findings suggest a potentially greater blood-damaging profile of the adult design. These differences are further exacerbated by the fact that the newborn pump has 38% fewer stagnation zones resulting in improved washout performance.

These findings align with prior observations by Wiegmann et al. [15], who reported that larger gaps within pump geometries can exacerbate flow disturbances and increase both vorticity and blood residence time. Additionally, the well-established relationship between elevated shear exposure and blood trauma, as documented in Fraser et al. and Thamsen et al. [31,33], supports our interpretation that the newborn-specific design, which minimizes these effects, may offer superior hemocompatibility. The improved washout performance observed in the newborn pump also resonates with literature emphasizing the importance of minimizing flow stasis to reduce thrombotic risk, given its role in Virchow's triad.

Clinically, the results underline the importance of using pumps specifically tailored for neonatal physiology rather than downscaling adult devices. The newborn pump demonstrates significantly lower regions of stasis, reduced high-stress exposure, and shorter blood residence times—factors that collectively suggest a lower risk of thrombus formation and blood damage. In neonatal patients, who are particularly vulnerable to complications from extracorporeal support, improving pump biocompatibility is critical. Our findings provide strong computational evidence in support of adopting neonatal-specific centrifugal pump designs in clinical practice.

5. Conclusion

The computational fluid dynamics analysis provided valuable insights into the hemodynamics of the adult and newborn pumps, highlighting differences in fluid dynamics features and their implications for

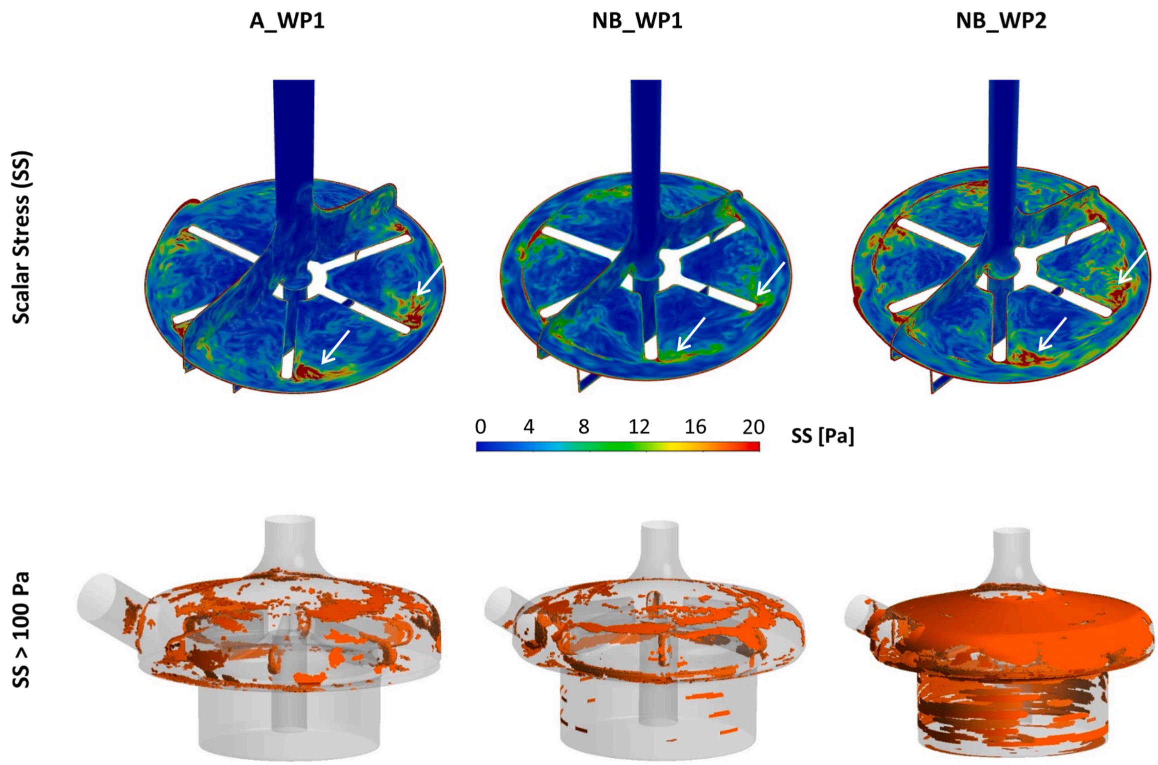

Fig. 7. Contour maps of scalar stress (top line) and volumes of fluid with scalar stress above 100 Pa (bottom line): comparison between A_WP1 (adult pump at working point WP1), NB_WP1 (newborn pump at working point WP1) and NB_WP2 (newborn pump at working point WP2). Arrows point to the areas on the suction side of the blades where elevated stress levels are observed.

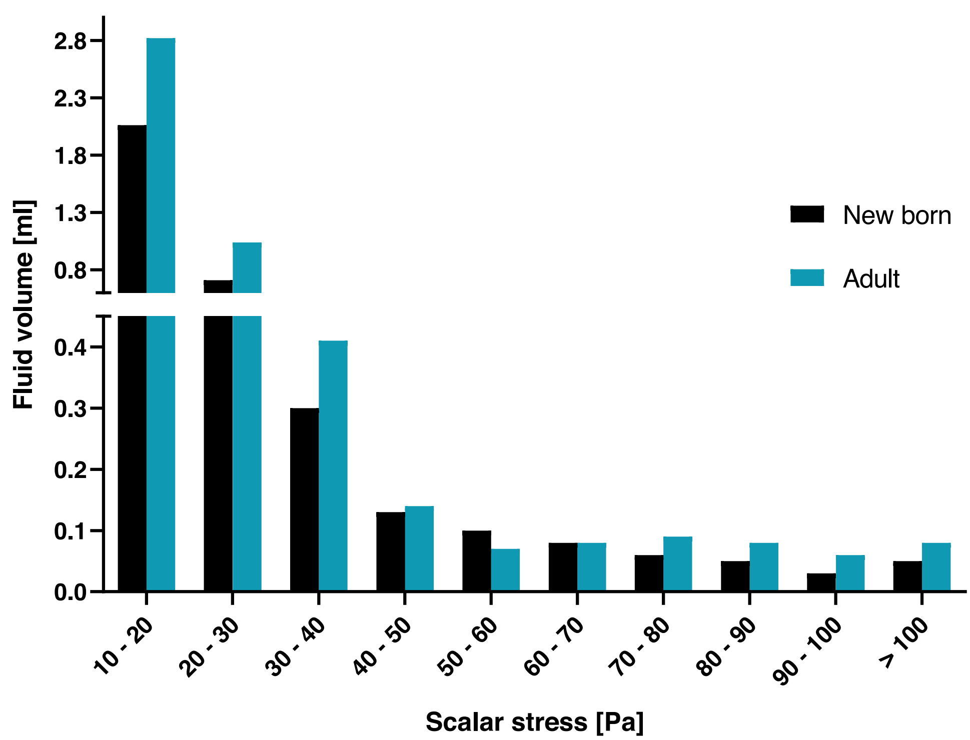

Fig. 8. Volumetric histograms of scalar stress above 10 Pa: comparison between adult and newborn pump at working point WP1.

clinical application. Overall, the newborn pump, in addition to having a reduced priming volume, also exhibits advantageous fluid dynamics features which support its application in paediatric cardiopulmonary bypass procedures instead of the adult pump. It demonstrates notably shorter exposure times, lower peak values of stresses and smaller volumes of fluid with critical values of stresses, suggesting a potentially reduced risk of blood damage. Moreover, the better washout performance reduces the risk of platelet aggregation and thrombus formation.

The improved hemodynamic performance of the newborn pump may translate into a lower risk of thrombus formation and hemolysis, which are critical concerns in neonatal patients requiring mechanical circulatory support. These improvements could contribute to enhanced biocompatibility and safety of the pump, potentially extending the duration of support and reducing complications. From a surgical perspective, the neonatal pump's design optimizations may be readily implemented into current extracorporeal life support systems with minimal adaptation, supporting its integration into existing clinical workflows.

Further research and validation studies are warranted to comprehensively assess the performance and thrombogenicity of the neonatal pump in clinical settings. Future studies should also include direct cross-comparisons with other existing neonatal devices to robustly contextualize and benchmark the proposed design within the current technological landscape.

Please state any sources of funding for your research

The study has been supported by Eurosets S.r.l., in the framework of an industrial research grant between Eurosets S.r.l. and Politecnico di Milano

Author contributions

S.B., A.R. and P.F. designed the study and directed the research. S.C. and F.B. carried out the CFD simulations and analysed the results. S.B., S. C., F.B. and A.R. interpreted the results. P.F. and M.C. performed the experimental measurements. S.B. and G.P. wrote the manuscript. S.B., F. C., G.P. and A.R. reviewed the manuscript. All authors critically approved the manuscript.

Ethical Approval

Work on human beings that is submitted to *Medical Engineering & Physics* should comply with the principles laid down in the Declaration of Helsinki; Recommendations guiding physicians in biomedical research involving human subjects. Adopted by the 18th World Medical Assembly, Helsinki, Finland, June 1964, amended by the 29th World Medical Assembly, Tokyo, Japan, October 1975, the 35th World Medical Assembly, Venice, Italy, October 1983, and the 41st World Medical Assembly, Hong Kong, September 1989. You should include information as to whether the work has been approved by the appropriate ethical committees related to the institution(s) in which it was performed and that subjects gave informed consent to the work.

Does your study involve human subjects?

No

If your study involves human subjects you MUST have obtained ethical approval.

Please state whether Ethical Approval was given, by whom and the relevant Judgement's reference number

Not required

Does your study involve animal subjects?

No

If your study involves animals you must declare that the work was carried out in accordance with your institution guidelines and, as appropriate, in accordance with the EU Directive 2010/63/EU. http://eur-lex.europa.eu/legal-content/EN/TXT/?uri=CELEX:32010L0063

Not required

Declaration of competing interest

Authors P.F. and M.C. are employed by Eurosets S.r.l., the manufacturer of the pumps investigated in the present study.

Funding

The work was funded by Eurosets S.r.l., in the framework of an industrial research grant between Eurosets S.r.l. and Politecnico di Milano.

References

[1] Sasaki T, Jikuya T, Aizawa T, Shiono M, Sakuma I, Takatani S, et al. A compact centrifugal pump for cardiopulmonary bypass. Artif Organs 1992 Dec;16(6):592–8.
[2] Bennett M, Horton S, Thuys C, Augustin S, Rosenberg M, Brizard C. Pump-induced haemolysis: A comparison of short-term ventricular assist devices. Perfusion 2004 Mar;19(2):107–11.
[3] Morgan IS, Codispoti M, Sanger K, Mankad PS. Superiority of centrifugal pump over roller pump in paediatric cardiac surgery: prospective randomised trial. Eur J Cardiothorac Surg 1998 May;13(5):526–32.
[4] Taenaka Y, Inoue K, Masuzawa T, Araki K, Sakaki M, Matsuo Y, et al. lnfluence of an impeller centrifugal pump on blood components in chronic animal experiments. ASAIO Journal 1992;38(3):M577–9.
[5] Zhang J, Gellman B, Koert A, Dasse KA, Gilbert RJ, Griffith BP, et al. Computational and experimental evaluation of the fluid dynamics and hemocompatibility of the CentriMag blood pump. Artif Organs 2006 Mar;30(3):168–77.
[6] Hijikata W, Sobajima H, Shinshi T, Nagamine Y, Wada S, Takatani S, et al. Disposable MagLev centrifugal blood pump utilizing a cone-shaped impeller. Artif Organs 2010 Aug;34(8):669–77.
[7] Condello I, Santarpino G, Serraino GF, Mastroroberto P, Speziale G, Nasso G. Magnetic levitation pump versus constrained vortex pump: a pilot study on the hemolysis effect during minimal invasive extracorporeal circulation. J Cardiothorac Surg 2021 Dec 1;16(1).
[8] Li P, Mei X, Ge W, Wu T, Zhong M, Huan N, et al. A comprehensive comparison of the in vitro hemocompatibility of extracorporeal centrifugal blood pumps. Front Physiol 2023 May 9;14:1136545.
[9] Biological evaluation of medical devices - Part 4: Selection of tests for interactions with blood. ISO; 2017.
[10] Hastings SM, Deshpande SR, Wagoner S, Maher K, Ku DN. Thrombosis in centrifugal pumps: Location and composition in clinical and in vitro circuits. Int J Artif Organs 2016 Jun 15;39(4):200–4.
[11] Chen Z, Zhang J, Li T, Tran D, Griffith BP, Wu ZJ. The impact of shear stress on device-induced platelet hemostatic dysfunction relevant to thrombosis and bleeding in mechanically assisted circulation. Artif Organs 2020 May 1;44(5):E201–13.
[12] Schibilsky D, Takatani S, Schibilsky B, Graf T, da Silva DM, Wendel HP, et al. Hemocompatibility of new magnetically-levitated centrifugal pump technology compared to the CentriMag adult pump. Sci Rep 2020 Dec 1;10(1).
[13] Graefe R, Henseler A, Steinseifer U. Multivariate assessment of the effect of pump design and pump gap design parameters on blood trauma. Artif Organs 2016 Jun 1;40(6):568–76.
[14] Mozafari S, Rezaienia MA, Paul GM, Rothman MT, Wen P, Korakianitis T. The effect of geometry on the efficiency and hemolysis of centrifugal implantable blood pumps. ASAIO Journal 2017 Jan 1;63(1):53–9.
[15] Wiegmann L, Boës S, de Zélicourt D, Thamsen B, Schmid Daners M, Meboldt M, et al. Blood pump design variations and their influence on hydraulic performance and indicators of hemocompatibility. Ann Biomed Eng 2018 Mar 1;46(3):417–28.
[16] Berg N, Fuchs L. Prahl Wittberg L. Flow characteristics and coherent structures in a centrifugal blood pump. Flow Turbul Combust 2019 Feb 15;102(2):469–83.
[17] Bozzi S, Vesentini S, Santus M, Ghelli N, Fontanili P, Corbelli M, et al. Fluid dynamics characterization and thrombogenicity assessment of a levitating centrifugal pump with different impeller designs. Med Eng Phys 2020 Sep 1;83:26–33.
[18] Huang B, Guo M, Lu B, Wu Q, Zuo Z, Liu S. Geometric optimization of an extracorporeal centrifugal blood pump with an unshrouded impeller concerning both hydraulic performance and shear stress. Processes 2021 Jul 1;9(7):1211.
[19] Luciani GB, Hoxha S, Torre S, Rungatscher A, Menon T, Barozzi L, et al. Improved outcome of cardiac extracorporeal membrane oxygenation in infants and children using magnetic levitation centrifugal pumps. Artif Organs 2016 Jan 1;40(1):27–33.
[20] Byrnes J, McKamie W, Swearingen C, Prodhan P, Bhutta A, Jaquiss R, et al. Hemolysis during cardiac extracorporeal membrane oxygenation: A case-control comparison of roller pumps and centrifugal pumps in a pediatric population. ASAIO Journal 2011 Sep;57(5):456–61.
[21] Gross-Hardt S, Hesselmann F, Arens J, Steinseifer U, Vercaemst L, Windisch W, et al. Low-flow assessment of current ECMO/ECCO2R rotary blood pumps and the potential effect on hemocompatibility. Crit Care 2019 Nov 6;23(1):348.
[22] Fiusco F, Broman LM, Wittberg LP. Blood pumps for extracorporeal membrane oxygenation: platelet activation during different operating conditions. ASAIO Journal 2022 Jan 1;68(1):79–86.
[23] Berdajs D, von Segesser LK, Maisano F, Milano G, Ferrari E. Performance characteristics of the new Eurosets magnetically suspended centrifugal pump. Perfusion 2021 Mar 1;36(2):183–9.

[24] Di Nardo M, Moreau A, Annoni F, Su F, Belliato M, Broman LM, et al. Evaluation of a new magnetically suspended centrifugal neonatal pump in healthy animals using a veno-venous extracorporeal membrane oxygenation configuration. Perfusion 2023 Sep 12:2676591231202380.

[25 Moin P, Mahesh K. Direct numerical simulation: a tool in turbulence research. Ann. Rev. Fluid Mech. 1998 Jan 1:539–78.

[26] Arzani A. Accounting for residence-time in blood rheology models: Do we really need non-Newtonian blood flow modelling in large arteries? J R Soc Interface 2018 Sep 1;15(146):0486.

[27] Good BC, Manning KB. Computational modeling of the Food and Drug Administration's benchmark centrifugal blood pump. Performance evaluation of a novel centrifugal blood pump. Artif Organs 2020 Jul 1;44(7):263–76.

[28] Meyer AD, Rishmawi AR, Kamucheka R, Lafleur C, Batchinsky AI, Mackman N, et al. Effect of blood flow on platelets, leukocytes, and extracellular vesicles in thrombosis of simulated neonatal extracorporeal circulation. J Thromb Haemost 2020 Feb;18(2):399–410.

[29] Bludszuweit C. Three-dimensional numerical prediction of stress loading of blood particles in a centrifugal pump. Artif Organs 1995 Jul;19(7):590–6.

[30] Hellums JD. Whitaker lecture: Biorheology in thrombosis research. Ann Biomed Eng 1993;22(5):445–55. 1994.

[31] Fraser KH, Zhang T, Taskin ME, Griffith BP, Wu ZJ. A quantitative comparison of mechanical blood damage parameters in rotary ventricular assist devices: Shear stress, exposure time and hemolysis index. J Biomech Eng 2012 Aug;134(8): 081002.

[32] ISO 18242. 2016 — Cardiovascular implants and extracorporeal systems — Centrifugal blood pumps. Geneva, Switzerland: International Organization for Standardization; 2016.

[33] Thamsen B, Blümel B, Schaller J, Paschereit CO, Affeld K, Goubergrits L, et al. Numerical analysis of blood damage potential of the HeartMate II and HeartWare HVAD rotary blood pumps. Artif Organs 2015 Aug 1;39(8):651–9.